On the clutch dynamics with the approximations of resulting contact forces (MAT140-15)

Igor Wojtunik, Michał Szewc, Grzegorz Kudra, Jan Awrejcewicz

Abstract: The aim of the work is to present effectiveness of numerical simulations of clutch with frictional contacts, elaborated by some of the current articles in the last few years. The friction models assumes full developed sliding and the classical Coulomb friction law on each element of the contact with general shape and any pressure distribution. Then special modification of the integral model of friction force and moment are proposed. The approximants based on Padé approximants and their generalizations. In the work the clutch dynamics with contacts forces model is presented. The system was simplified to friction disk on rotating master disk. Two different configurations are investigated: coaxial and non-coaxial arrangement of the two disks. For the appropriate rotations speed, the system of non-coaxial arrangement can exhibit the ability to self-centering. The models based on generalizations of Padé approximants are compared with the simulation results obtained by the use of approximants based on Taylor's expansion and models with exact integral expressions for friction force and torque components.

1. Introduction

There are some ways of examination of systems with resultant contact forces. They identify difficulties with correct numerical simulation. Usual integral models are complex. Such situation requires a new method i.e. discretization or approximations.

In 1962, Contensou indicated in his paper [1] the integral model of the resultant friction force. It assumes fully developed sliding and the classical Coulomb friction law on each element of the contact area. In this integral model, circular area and Hertzian contact pressure distribution were applied. Some other authors presented special approximations of expressions for friction force and moment based on Padé approximants [2]. For the purpose of numerical simulations, these models were more convenient and suitable. In the paper [3], the types of generalizations of these approximants were presented. The models were extended with elliptical contact area. Such generalization increased their ability to match experimental data or the integral models. The models were applied in simulation of the Celtic stone [4]. Other example of applications is given in the work [5], where authors attempted to shape the trajectory of billiard ball.

In 2009, Fidlin and Stamm investigated radial dynamics of systems [6], commonly encountered in the clutch and many other applications. Two systems were the objects of their study: pin-on-the-

disk and disk-on-the-disk. To simplify the expressions of friction force and moment, Taylor's expansion was applied. The model was used to study the stability of equilibriums.

Authors of the present work compared three models of resultant contact forces: exact integral expressions for friction force and torque components, approximations based on generalizations of Padé approximants and Taylor's expansions. Then, the system with friction disk on rotating master disk was analyzed and simulated.

2. Modeling of contact forces

Let us focused on to the contact pressure distribution. In the Cartesian coordinate system *Axyz*, we consider dimensionless ring contact area *F* (figure 1). Axes *x* and *y* lie in the contact plane. The dimensionless length is obtained by dividing actual length by $\hat{a}$, which is radius of real contact.

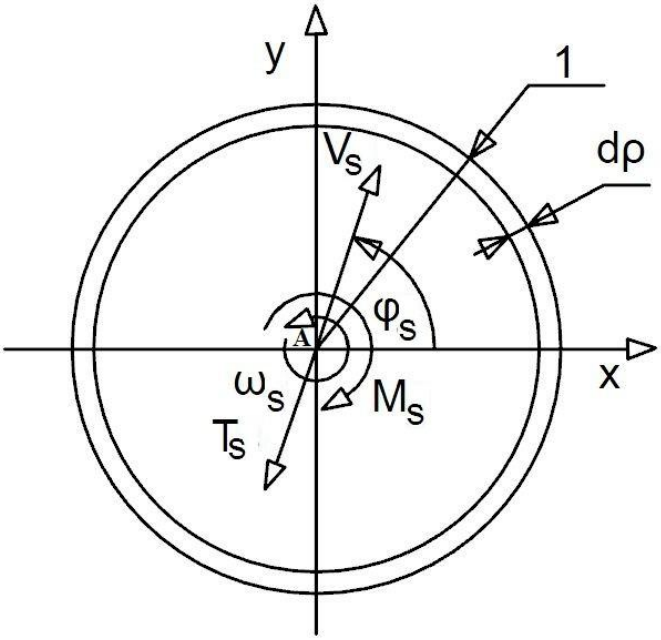

Figure 1. The ring contact area

The non-dimensional thickness of the contact ring is elementary small $d\rho \to 0$ and its real value can be presented as follows:

$$d\hat{\rho} = \hat{a}d\rho. \tag{1}$$

The real contact pressure distribution is assumed to be constant and reads [3,4]:

$$\hat{\sigma}(x,y)=\frac{\hat{N}}{\hat{F}}=\frac{\hat{N}}{2\pi\hat{a}^2 d\rho}. \tag{2}$$

In equations (2) there are used the following notations: $\hat{N}$ - normal component of real resultant force loading the contact, $\hat{\sigma}(x,y)$ - real contact pressure, $\hat{F}$ - real contact area. Non-dimensional contact pressure distribution is defined as:

$$\sigma(x,y)=\hat{\sigma}(x,y)\frac{\hat{a}^2}{\hat{N}}=\frac{1}{2\pi d\rho}. \tag{3}$$

We assumed a fully developed sliding. The relative motion of the two bodies is considered as a plane motion of rigid bodies. It is characterised by the non-dimensional angular and linear velocity, respectively: $\boldsymbol{\omega}_S=\hat{\boldsymbol{\omega}}_S=\omega_S\mathbf{e}_Z$ and $\mathbf{v}_S=\hat{\mathbf{v}}_S/\hat{a}=v_{Sx}\mathbf{e}_X+v_{Sy}\mathbf{e}_Y$, where $\hat{\mathbf{v}}_S$ is the real linear sliding velocity in the center *A*, $\hat{\boldsymbol{\omega}}_S$ is the real angular sliding velocity, and $\mathbf{e}_X$, $\mathbf{e}_Y$, $\mathbf{e}_Z$ are the unit vectors of the corresponding axes. Each element *dF* is under action of elementary friction force $d\mathbf{T}=-\sigma(x,y)\,dF\,\mathbf{v}_P/\|\mathbf{v}_P\|$ and moment $d\mathbf{M}=\boldsymbol{\rho}\times d\mathbf{T}=d\hat{\mathbf{M}}/(\hat{a}\,\mu\hat{N})$, where $\mathbf{v}_P$ stands for dimensionless, local velocity of sliding and μ is dry friction coefficient. Total values of contact forces are equal to: $\mathbf{T}_S=-T_{Sx}\mathbf{e}_X-T_{Sy}\mathbf{e}_Y$ and $\mathbf{M}_S=-M_S\mathbf{e}_Z$, where:

$$\begin{aligned}
T_{Sx}&=\iint_F\sigma(x,y)\frac{(v_{Sx}-\omega_S y)}{\sqrt{(v_{Sx}-\omega_S y)^2+(v_{Sy}+\omega_S x)^2+\varepsilon_t^2}}dxdy,\\
T_{Sy}&=\iint_F\sigma(x,y)\frac{(v_{Sy}+\omega_S x)}{\sqrt{(v_{Sx}-\omega_S y)^2+(v_{Sy}+\omega_S x)^2+\varepsilon_t^2}}dxdy,\\
M_S&=\iint_F\sigma(x,y)\frac{\omega_S(x^2+y^2)+v_{Sy}x-v_{Sx}y}{\sqrt{(v_{Sx}-\omega_S y)^2+(v_{Sy}+\omega_S x)^2+\varepsilon_t^2}}dxdy.
\end{aligned} \tag{4}$$

It is an integral expression with additional, small parameter ε_t to avoid singularity. It is related to the lack of the relative motion. The real quantities are equal to: $\hat{\mathbf{T}}_S=\mu\hat{N}\,\mathbf{T}_S$ and $\hat{\mathbf{M}}_S=\hat{a}\mu\hat{N}\mathbf{M}_S$. In order to apply (4) in the simulation, the change of coordinate system from Cartesian coordinate system *Axyz* to pole coordinate system was essential. It is presented in Figure 2. The following

relation was implemented: $x = \rho\cos\alpha$, $y = \rho\sin\alpha$ and $dF = dxdy = \rho d\alpha d\rho$, leading to the following form of integrals:

$$T_{sx} = \frac{1}{2\pi}\int_0^{2\pi} \frac{\left(v_{sx} - \omega_s \rho\sin\alpha\right)}{\sqrt{\left(v_{sx} - \omega_s\,\rho\sin\alpha\right)^2 + \left(v_{sy} + \omega_s\rho\cos\alpha\right)^2 + \varepsilon_t^2}} d\alpha\,,$$

$$T_{sy} = \frac{1}{2\pi}\int_0^{2\pi} \frac{\left(v_{sy} + \omega_s \rho\cos\alpha\right)}{\sqrt{\left(v_{sx} - \omega_s\rho\sin\alpha\right)^2 + \left(v_{sy} + \omega_s\rho\cos\alpha\right)^2 + \varepsilon_t^2}} d\alpha\,, \tag{5}$$

$$M_s = \frac{1}{2\pi}\int_0^{2\pi} \frac{\omega_s\left(\rho^2\cos^2\alpha + \rho^2\sin^2\alpha\right) + v_{sy}\rho\cos\alpha - v_{sx}\rho\sin\alpha}{\sqrt{\left(v_{sx} - \omega_s\rho\sin\alpha\right)^2 + \left(v_{sy} + \omega_s\rho\cos\alpha\right)^2 + \varepsilon_t^2}} d\alpha\,.$$

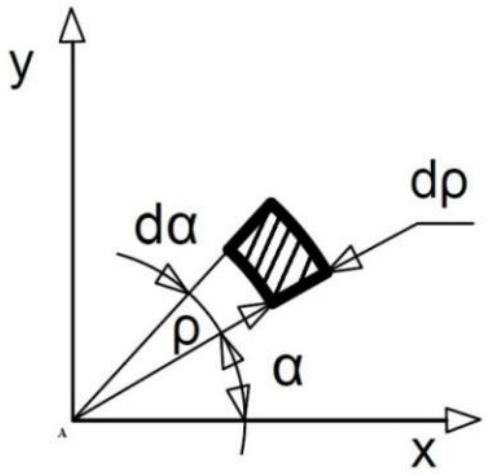

Figure 2. The ring contact area

For a fact this expression (3) has a complex integral form where the simulation and the numerical solutions are time consuming. It is inconvenient, and can be avoided by implementing approximate form of resultant contact forces. Based on special modifications of Padé approximants [3] we get:

$$T_{sx}^{(I)} = \frac{v_{sx} - b_T c_{0,1,1}^{(x,y)}\omega_s}{\sqrt{\left(|v_s|^{m_T} + b_T^{m_T}|\omega_s|^{m_T}\right)^{2m_T^{-1}} + \varepsilon_t^2}},$$

$$T_{sy}^{(I)} = \frac{v_{sy} + b_T c_{1,0,1}^{(x,y)} \omega_s}{\sqrt{\left(|v_s|^{m_T} + b_T^{m_T} |\omega_s|^{m_T} \right)^{2m_T^{-1}} + \varepsilon_t^2}}, \tag{6}$$

$$M_s^{(I)} = \frac{b_M c_{0,0,-1}^{(x,y)} \omega_s - c_{0,1,0}^{(x,y)} v_{sx} + c_{1,0,0}^{(x,y)} v_{sy}}{\sqrt{\left(b_M^{m_M} |\omega_s|^{m_M} + |v_s|^{m_M} \right)^{2m_M^{-1}} + \varepsilon_t^2}}.$$

where

$$c_{i,j,k}^{(x,y)} = \iint_F x^i y^j \left(x^2 + y^2 \right)^{-\frac{k}{2}} \sigma(x,y)\, dxdy\,. \tag{7}$$

The integral (6) are equal to the corresponding integral ones for $\varepsilon_t = 0$ and $v_s = \sqrt{v_{sx}^2 + v_{sy}^2} = 0$ or $\omega_s = 0$. Optimization process, with the approximate model being adjusted to the integral components or real experimental data, is based on finding appropriate, constant parameters b_T, m_T, b_M and m_M. For the ringed contact area and the contact pressure distribution (2), the integrals occurring in equations (6) read:

$$c_{0,1,1}^{(x,y)} = c_{1,0,1}^{(x,y)} = c_{0,1,0}^{(x,y)} = c_{1,0,0}^{(x,y)} = 0, \quad c_{0,0,-1}^{(x,y)} = 1. \tag{8}$$

3. Determination of the parameters of the model of the resultant contact forces

The proposed approximation based on modification of Padè approximants was adjusted to the corresponding integral components and Taylor's expansion from the work [6]. The following change variables was introduced in order to reduce the number of variables and simplify the optimization process:

$$v_s = \lambda_s \cos\theta_s, \quad \omega_s = \lambda_s \sin\theta_s, \quad v_{sx} = v_s \cos\varphi_s, \quad v_{sy} = v_s \sin\varphi_s, \tag{9}$$

where

$$\lambda_s = \sqrt{v_s^2 + \omega_s^2}\,.$$

Relations (9) were applied to expressions (4), (6) and Taylor's expansion, and the optimal parameters of b_T, m_T, b_M, m_M were found, fitting the corresponding functions on the representative integral $-\pi/2 < \theta_S < \pi/2$.

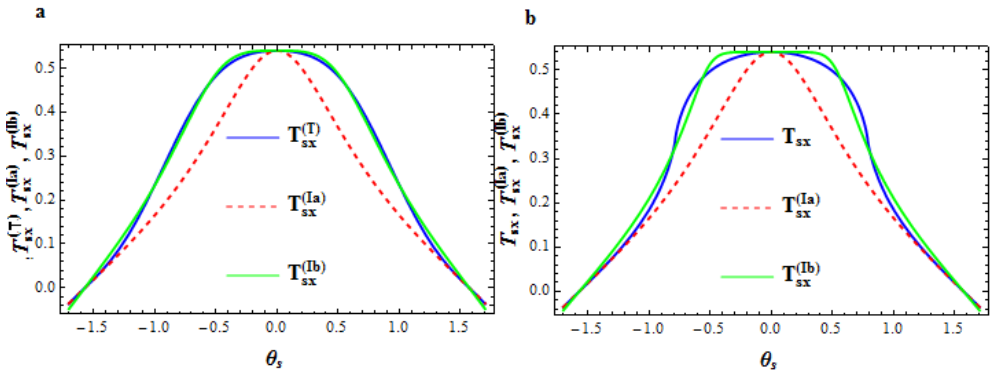

Figure 3. Friction force T_S in direction *x*

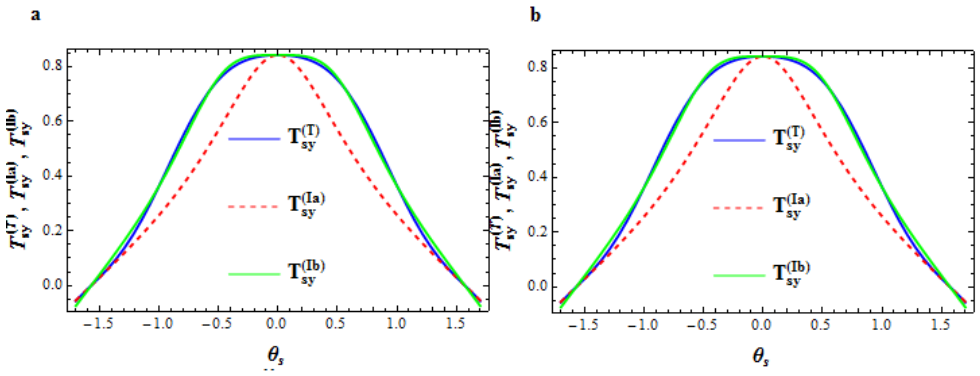

Figure 4. Friction force T_S in direct**io**n *y*

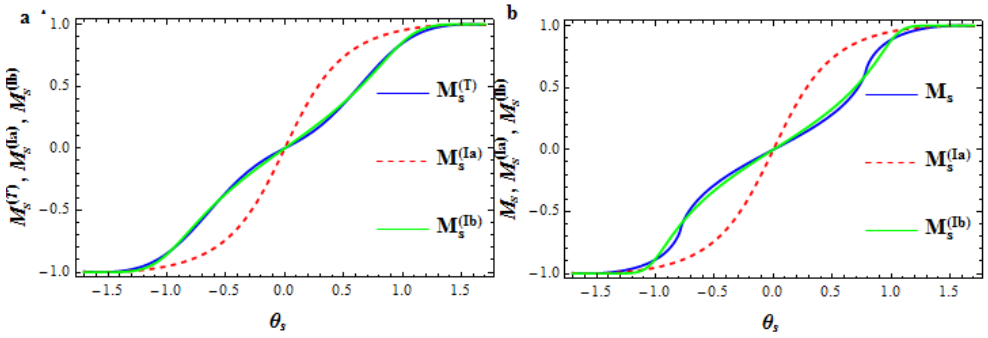

Figure 5. Moment M_S

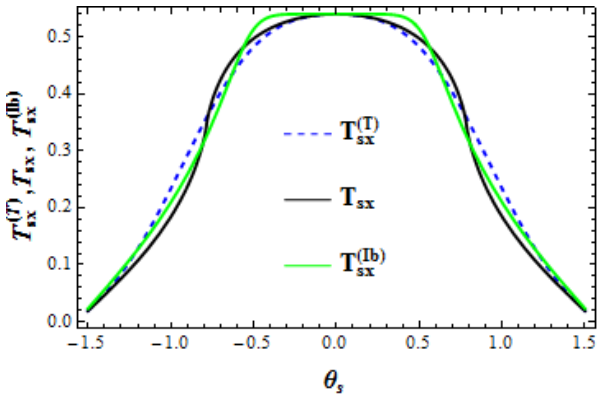

Figure 6. Comparison of friction force T_{SX}

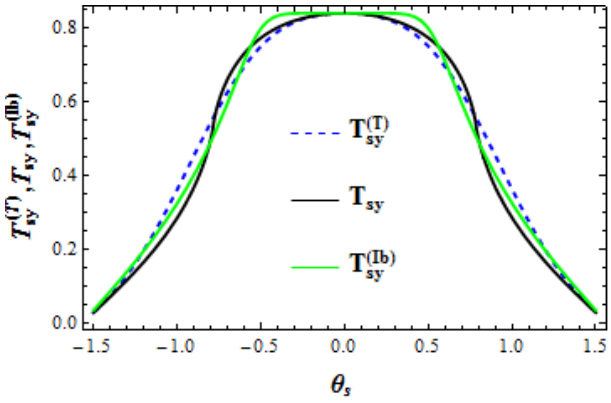

Figure 7. Comparison of friction force T_{Sy}

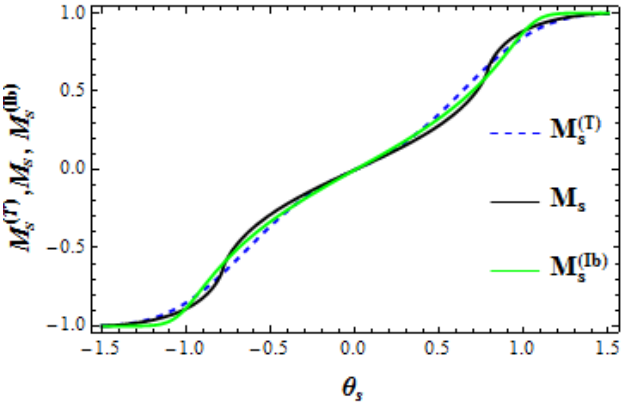

Figure 8. Comparison of moment M_S

Figures 3, 4 and 5 present resultant contact forces with parameters b_T=m_T=b_M=m_M=2 (Ia) and optimal parameters (Ib) to fit to Taylor's expansion (a): b_T=1.47, m_T=3.6, b_M=0.68, m_M=3.86 and integral model (b): b_T=1.66, m_T=7.57, b_M=0.61, m_M=7.59. The simulation was performed for φ_S = 1 rad. Figures 6, 7 and 8 present comparison of all resultant contact forces with (Ib) fitted to the integral model .

4. Simulation of disk-on-the-disk system

Presented clutch was simplified to disk-on-the-disk system, which can be seen in figure 6. This is a friction disk laying on the rotating master disk. The two bodies were coupling on the ring area.

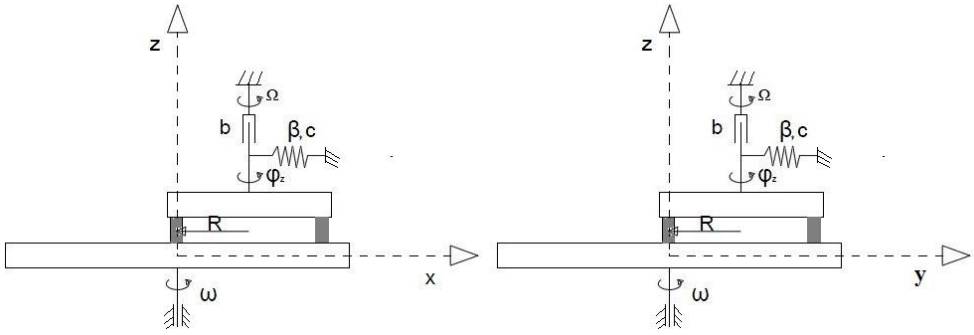

Figure 9. Disk-on-the-disk system from paper [6]

The following notation was used: $\hat{\mathbf{T}}_S$ – the resultant friction force acting at the contact center *A*; $\hat{\mathbf{N}}$ - the normal reaction acting on the disk; $\hat{\boldsymbol{\omega}}_S$ – angular sliding velocity; $\hat{\mathbf{M}}_S$ – moment of friction forces; $\hat{\mathbf{v}}_\mathbf{S}$ - linear sliding velocity at the point *A*; $R=\hat{a}$ – radius of contact ring; *m* – mass of the friction disk; *J* – moment of inertia of friction disk; ω - angular velocity of master disk; Ω – constant angular velocity of infinity mass connected to the friction disk by element with damping coefficient *b*; β, *c* – damping coefficient and stiffness of elasto-damping elements supporting friction disk in directions *x* and *y*; x_0 – position of spring relaxation in the direction *x*.

The analyzed system has three degree of freedom and the governing equations reads:

$$\begin{aligned}
\frac{d^2x}{dt^2} &= -\frac{\hat{T}_{sx}}{m} - \frac{\beta}{m}\frac{dx}{dt} - \frac{c}{m}(x - x_0), \\
\frac{d^2y}{dt^2} &= -\frac{\hat{T}_{sy}}{m} - \frac{\beta}{m}\frac{dy}{dt} - \frac{c}{m}y, \\
\frac{d^2\varphi_z}{dt^2} &= \frac{\hat{M}_S}{J} - \frac{b}{J}\left(\frac{d\varphi_z}{dt} - \Omega\right).
\end{aligned} \tag{10}$$

The relations between the corresponding kinematic variables occurring in (10) and models (4) and (6) are as follows:

$$\begin{aligned}
\hat{v}_{sx} &= \dot{x} + \omega y, \quad v_{sx} = \frac{\hat{v}_{sx}}{R}, \\
\hat{v}_{sy} &= \dot{y} - \omega x, \quad v_{sy} = \frac{\hat{v}_{sy}}{R}, \\
\hat{v}_s &= \sqrt{\hat{v}_{sx}^{\,2} + \hat{v}_{sy}^{\,2}}, \\
v_s &= \sqrt{v_{sx}^{\,2} + v_{sy}^{\,2}}, \\
\hat{\omega}_s &= \omega_s = \omega - \dot{\varphi}_z.
\end{aligned} \tag{11}$$

Then one can use the integral model (4), taking to account the following relations between real and non-dimensional quantities: $\hat{\mathrm{T}}_{sx} = \mu N \mathrm{T}_{sx}$, $\hat{\mathrm{T}}_{sy} = \mu N \mathrm{T}_{sy}$, and $\hat{\mathrm{M}}_S = R\mu N \mathrm{M}_\mathrm{S}$. The integral

components T_{sx}, T_{sy} and M_s can be replaced by the corresponding approximants $T_{sx}^{(I)}$, $T_{sy}^{(I)}$ and $M_s^{(I)}$ (6), or Taylor's expansions proposed in the work [6]:

$$T_{sx}^{(T)} = \frac{1}{\bar{v}_r}\frac{v_{sx}}{R}(1-\frac{R^2\omega_s^2}{2\bar{v}_r^2}+\frac{3}{4}\phi),$$

$$T_{sy}^{(T)} = \frac{1}{\bar{v}_r}\frac{v_{sy}}{R}(1-\frac{R^2\omega_s^2}{2\bar{v}_r^2}+\frac{3}{4}\phi), \qquad (12)$$

$$M_s^{(T)} = \frac{1}{\bar{v}_r R}\omega_s(1-\frac{\left(\frac{v_s}{R}\right)^2}{2\bar{v}_r^2}+\frac{3}{4}\phi),$$

where

$$\bar{v}_r = \sqrt{\left(\frac{v_{sx}}{R}\right)^2+\left(\frac{v_{sy}}{R}\right)^2+R^2\omega_s^2},$$

$$\phi = \frac{R^2(\omega-\dot{\varphi})^2}{\bar{v}_r^2}\frac{\left(\frac{v_s}{R}\right)^2}{\bar{v}_r^2}.$$

To simulate the system, the following parameters and initial conditions were used: t = 20 s; R = 1 m; μN = 0.225 N; J = 1 kg/m^3; m = 1 kg; Ω = 1.25 rad/s; β = 0.5 s*N/m; c = 1 N/m; b = 0.015 s*N/m; ε_t = 0.1; x_0 = 0.1 m; $x(0) = y(0) = \varphi_Z(0) = \dot{x}(0) = \dot{y}(0) = \dot{\varphi}_Z(0) = 0$. Figure 7 a-b presents three diagrams with simulations performed with the use of integral components of resultant contact forces and their two approximations: 7 a – approximant (I) fitted to Taylor's expansions (T) with the parameter ω = 2.5 rad/s, 7 b – approximant (I) fitted to integral model with the parameter ω = 0.8 rad/s. Figure 7 c-f shows trajectory of friction disk with approximants $T_{sx}^{(Ib)}$, $T_{sy}^{(Ib)}$, $M_s^{(Ib)}$ and $x(0)$ = 0.0001 m. Figure 7 c-d presents coaxial arrangement of disk (x_0 = 0 m) for ω = 0.8 rad/s (see figure 7 c) and ω = 2.5 rad/s, (see figure 7 d). Figure 7 e-f presents non-coaxial arrangement of disk (x_0=0.1m) for ω= 0.8 rad/s (see figure 7 e) and ω = 2.5 rad/s, (see figure 7 f). The simulation time was 700 seconds.

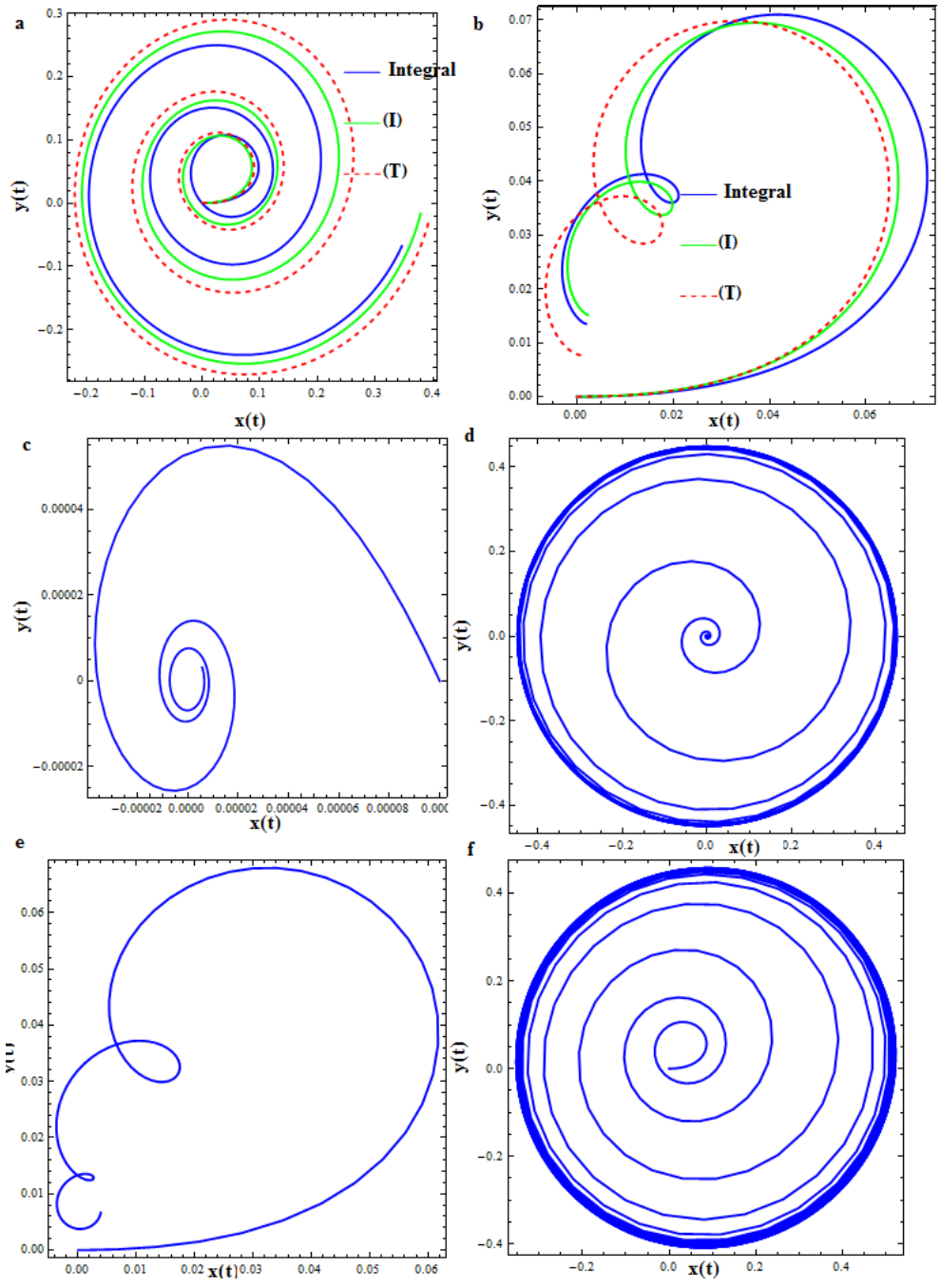

Figure 10. Simulation of disk-on-the-disk system.

5. Conclusions

The work present flexibility of the proposed model of resultant contact forces based on modifications of Padè approximant. It can be used to simulate disk-on-the-disk system and to study the stability of equilibriums. Such form of the model is more convenient and less time consuming. It gives the possibility of longer simulation. The paper presents simulations of disk-on-the-disk system. Its dynamics maps the clutch behavior in some aspects. It confirms typical behavior of self-centering of the system for low rotation speeds.

Acknowledgments

This work has been supported by the Polish National Science Centre, MAESTRO 2, No. 2012/04/A/ST8/00738.

References

[1] Contensou, P., *Couplage entre frottement de glissement et de pivotement dans la téorie de la toupe*, In: Ziegler H. (Ed.), Kreiselprobleme Gyrodynamic, IUTAM Symposium Celerina, Springer-Verlag, Berlin, 1962, pp. 201-216.

[2] Zhuravlev, V.P., The model of dry friction in the problem of the rolling of rigid bodies, *Journal of Applied Mathematics and Mechanics*, 62(5), 1998, pp. 705-710.

[3] Kudra, G., Awrejcewicz, J., "Application and experimental validation of new computational models of friction forces and rolling resistance", *Acta Mechanica*, 2015, pp. 2831-2848.

[4] Kudra, G., Awrejcewicz, J., "Approximate modelling of resulting dry friction forces and rolling resistance for elliptic contact shape", *European Journal of Mechanics A/Solids*, 42, 2013, pp. 358-375.

[5] Kudra, G., Szewc, M., Wojtunik, I., Awrejcewicz J. Shaping the trajectory of the billiard ball with approximations of the resultant contact forces., *3rd Int. Conference on Mechatronics — Ideas for Industrial Applications*, May 11-13, Gdansk, 2015

[6] Fidlin , W. Stamm, On the radial dynamics of friction disks, *European Journal of Mechanics A/Solids*, 2009

Wojtunik Igor, M.Sc. (Ph.D. student): Lodz University of Technology, Department of Automation, Biomechanics and Mechatronics, Stefanowskiego 1/15, 90-924 Lodz, Poland (igor.wojtunik@dokt.p.lodz.pl). The author gave a presentation of this paper during one of the conference sessions.

Szewc Michal, M.Sc. (Ph.D. student): Lodz University of Technology, Department of Automation, Biomechanics and Mechatronics, Stefanowskiego 1/15, 90-924 Lodz, Poland (michal.szewc@dokt.p.lodz.pl).

Kudra Grzegorz, Ph.D.: Lodz University of Technology, Department of Automation, Biomechanics and Mechatronics, Stefanowskiego 1/15, 90-924 Lodz, Poland (grzegorz.kudra@p.lodz.pl).

Awrejcewicz Jan, Professor: Lodz University of Technology, Department of Automation, Biomechanics and Mechatronics, Stefanowskiego 1/15, 90-924 Lodz, Poland (jan.awrejcewicz@p.lodz.pl).